J. Arbi
I. Slama-Belkhodja

J. Electrical Systems 4-1 (2008): 51-59

Regular paper

Direct Torque Control in presence of Current sensor failure in Variable Speed Wind System: Effect analysis, detection and control reconfiguration

This paper presents a study of current sensor failure in a Direct Torque Control applied to a Double Fed Induction Generator based Variable Speed Wind System. The effect of scaling and offset current sensor errors is discussed through sensibility analysis. A control reconfiguration is then proposed to remedy this sensor failure. Simulation results emphasize the good performances of the proposed current sensor fault tolerant control.

Key words: DFIG, sensor fault, Wind System, sensibility analysis, control reconfiguration

1. INTRODUCTION

In recent years, the amount of distributed renewable generation systems, mainly wind farms, demand continuous improving of efficiency and system reliability. Actually, grid connected wind farms present many issues that have been discussed in literature whether in healthy or faulty modes. A lot of works have treated the fault ride through capability of wind turbines in case of network failures [1], [2],[3]. Besides voltage sags, other faults may affect the wind system and must be treated as well for the sake of reliability improvement. This work deals with current sensor faults in a Doubly Fed Induction Generator (DFIG) based Variable Speed Wind System (VSWS). This system configuration uses a wound rotor asynchronous generator with a four quadrant ac-to-ac converter connected to rotor windings while stator winding are directly connected to the grid [4]. The redundancies inherent to this system structure are exploited in order to remedy current sensor failures. The problem of current sensors faults in Electrical Drives has been treated in different works. In [5], authors studied this problem for synchronous generator with Direct Torque Control (DTC) algorithm and in [6] with the same control but for asynchronous motor. In [7] and [8], the problem is discussed for asynchronous motor with vector control.

The originality of this paper is the sensibility analysis of the control algorithm namely (DTC) [9] to sensor faults and the reconfiguration of the control based on the redundancy offered by the wind system under study.

The paper is organized as follows: the second section describes the system under study and the control algorithm. The third section analyzes the effect of current sensor failure, with a sensibility analysis and simulation results. The last part presents the proposed self-reconfiguration system control, with a fault detection and isolation (FDI) method, in such a way that the generator continues working safely. Simulation results show the successful operation of the proposed system.

The current failures considered are the two major failure types that can affect the hall effect closed loop technology current sensors [10],[11] commonly used in VSWS : offset and scaling errors.

L.S.E, Ecole Nationale d'Ingénieurs de Tunis, BP 37, Le Belvédère, Tunis,
Tel: (216) 71 87 47 00- Fax: (216) 71 87 47 29 e-mail: jihen_alarbi@yahoo.fr, **Ilhem.slama@enit.rnu.tn**

2. SYSTEM AND CONTROL DESCRIPTION

The power configuration of the VSWS under study is depicted in Figure 1.a. It consists in a DFIG connected to the grid directly on the stator side, and via a back-to-back converter on the rotor side.

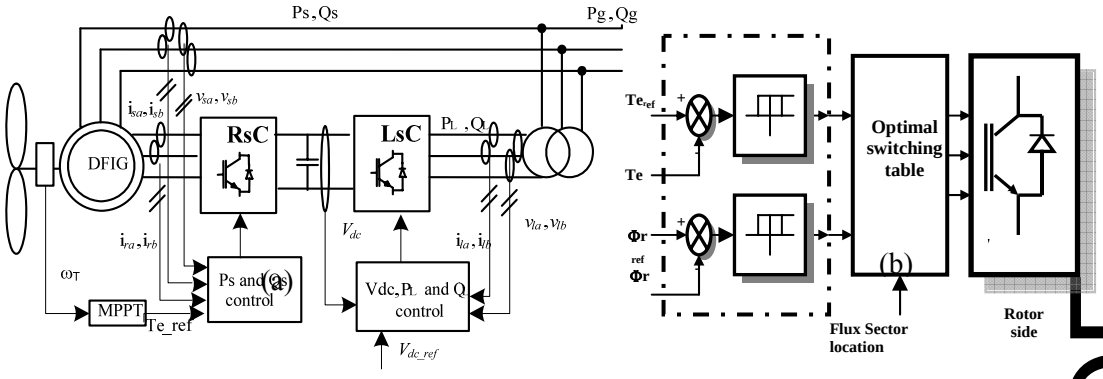

Figure 1: (a) Power configuration of the DFIG wind system (b) Principle of Direct Torque Control

The Rotor side Converter (RsC) ensures a decoupled active and reactive stator power control, Ps and Qs, according to the reference torque delivered by the Maximum Power Point Tracking control (MPPT). The Line side Converter (LsC) controls the power flow exchange with the grid via the rotor, by maintaining the dc bus at a constant voltage level and by imposing the reactive power Q_L at zero [12]. This paper focuses on RsC control. The control algorithm used for this converter is the Direct Torque Control (DTC) (see Figure 1.b).

DTC is based on the control of flux and torque directly using two hysteresis controllers.

The electromagnetic torque expression used for the DTC is the well known one given by (1), function of the stator and rotor flux linkages and the angle γ between them:

$$T_{em} = \frac{3}{2} p \frac{M_{sr}}{\sigma . L_s . L_r} \Phi_r . \Phi_s . \sin \gamma \qquad (1)$$

Where σ is the leakage factor, p the pole pair number, M_{sr}, L_s, L_r are the inductances per phase. The DTC applied to the rotor side converter of the DFIG is based on the same principle as for squirrel cage induction generators, with the difference that, in the wind system studied, the rotor flux is regulated: the stator flux is constant in magnitude and frequency since the stator is directly connected to the grid. So the torque is controlled through the control of the magnitude and angle of rotor flux. The DTC strategy is implemented as a look-up table, which gives the switching states of the power semi-conductors depending on the logic outputs of flux and torque hysteresis controllers and the position of the flux vector. The switching pattern determines the voltage vector to apply to the rotor in order to make the desired action on the magnitude and angle of the rotor flux vector [12].The control needs torque and flux feedbacks. Flux estimation uses measured stator and rotor currents. The equations of rotor flux components in the fixed $\alpha\beta$ reference frame, linked to the stator, are given below, where θ is the angle between a same stator and rotor phase:

$$\begin{cases}\Phi_{r\alpha} = L_r.I_{r\alpha} + M_{sr}.\left(I_{s\alpha}.\cos\theta + I_{s\beta}.\sin\theta\right)\\ \Phi_{r\beta} = L_r.I_{r\beta} + M_{sr}.\left(I_{s\beta}.\cos\theta - I_{s\alpha}.\sin\theta\right)\end{cases} \quad (2)$$

It can be noticed that no integration is needed for the calculation of the flux, which represents an important advantage especially from a numeric implementation point of view.

Magnitude of rotor flux is calculated using the $\alpha\beta$ components (equation (2)) as follows:

$$\left|\Phi_r\right| = \sqrt{\Phi^2_{r\alpha} + \Phi_{r\beta}{}^2} \quad (3)$$

The actual sector K which represents the location of rotor flux vector is calculated using estimated $\Phi_{r\alpha}$ and $\Phi_{r\beta}$.

Torque estimation uses estimated flux components and measured rotor currents as follows:

$$T_{em} = p.\left(\Phi_{r\alpha}.I_{r\beta} - \Phi_{r\beta}.I_{r\alpha}\right) \quad (4)$$

The power-invariant form of the phase transformation (equation (5)) provides both stator and rotor current components in respectively the reference frame fixed to stator and the reference frame linked to the rotor (The subscript "x" corresponds to "*s*" for stator quantities and to "*r*" for rotor ones).

$$\begin{cases}X_{x\alpha} = \sqrt{\frac{3}{2}}X_{x1}\\ X_{x\beta} = \frac{1}{\sqrt{2}}.(X_{x1} + 2X_{x2})\end{cases} \quad (5)$$

3. SENSIBILITY ANALYSIS

Two major sensor faults are treated in this work namely offset and scaling faults. The general equations characterizing a current sensor fault in the studied algorithm (DTC) are the error expressions of the rotor flux (calculated through the estimated components of the rotor flux in the $\alpha\beta$ stator frame) and electromagnetic torque. The study focuses on these two variables (torque and flux) mainly because the robustness of the control depends on their estimation. In the following equations ((6) and (7)), flux and torque error general expressions are calculated in the case where the fault affects stator sensors and the study can be extended in the same way when rotor sensors are faulty. Equation (6) is obtained using (2) and the error expression of $\Delta I_{s\alpha}$ and $\Delta I_{s\beta}$ as a function of ΔI_{s1}, ΔI_{s2} and ΔI_{s3} .

$$\begin{cases}\Delta\Phi_{r\alpha} = M_{sr}.\sqrt{\frac{3}{2}}.\left[\Delta I_{s1}.\cos\theta + \Delta I_{s2}.\cos\left(\theta - \frac{2\pi}{3}\right) + \Delta I_{s3}.\cos\left(\theta + \frac{2\pi}{3}\right)\right]\\ \Delta\Phi_{r\beta} = -M_{sr}.\sqrt{\frac{3}{2}}.\left[\Delta I_{s1}.\sin\theta + \Delta I_{s2}.\sin\left(\theta - \frac{2\pi}{3}\right) + \Delta I_{s3}.\sin\left(\theta + \frac{2\pi}{3}\right)\right]\end{cases} \quad (6)$$

$$\Delta T_{em} = p[\Delta\Phi_{r\alpha}.I_{r\beta} - \Delta\Phi_{r\beta}.I_{r\alpha}] \tag{7}$$

The two sensor faults cases are studied independently: offset error and scaling error.

3.1. Offset error

Equation (8) expresses the error when the current sensors present an offset fault.

$$\Delta I_{si} = k_i \tag{8}$$

Where $i \in \{1,2,3\}$ and k_i is a scalar constant corresponding to the offset in the i[th] sensor. Substituting (8) in (6), flux error is expressed in (9).

$$\begin{cases} \Delta\Phi_{r\alpha} = M_{sr}.\sqrt{\frac{3}{2}}.\left[k_1.\cos\theta + k_2.\cos\left(\theta - \frac{2\pi}{3}\right) + k_3.\cos\left(\theta + \frac{2\pi}{3}\right)\right] \\ \Delta\Phi_{r\beta} = -M_{sr}.\sqrt{\frac{3}{2}}.\left[k_1.\sin\theta + k_2.\sin\left(\theta - \frac{2\pi}{3}\right) + k_3.\sin\left(\theta + \frac{2\pi}{3}\right)\right] \end{cases} \tag{9}$$

In this study, only one sensor is supposed to be faulty, which is the most common case (here sensor of phase 1, so $k_1 \neq 0$ and $k_2 = k_3 = 0$). Equation (9) is then simplified in this case, and $\Delta\Phi_{r\alpha}$ and $\Delta\Phi_{r\beta}$ are given in (10).

$$\begin{cases} \Delta\Phi_{r\alpha} = \sqrt{\frac{3}{2}}.M_{sr}.k_1.\cos\theta \\ \Delta\Phi_{r\beta} = -\sqrt{\frac{3}{2}}.M_{sr}.k_1.\sin\theta \end{cases} \tag{10}$$

Stator currents can be expressed by :

$$\begin{cases} I_{s1} = |I_s|.\sin\theta_s \\ I_{s2} = |I_s|.\sin\left(\theta_s - \frac{2\pi}{3}\right) \\ I_{s3} = |I_s|.\sin\left(\theta_s + \frac{2\pi}{3}\right) \end{cases} \tag{11}$$

Error on rotor flux modulus can be deduced from (2), (10) and (11):

$$\Delta|\Phi_r| \approx \sqrt{\frac{3}{2}}.M_{sr}.k_1.\cos\theta_s \tag{12}$$

Using (7) and (10), the error on electromagnetic torque is expressed by (13).

$$\Delta T_{em} = -\frac{3}{2}.M_{sr}.k_1.\left|I_r\right|.\cos\theta_s \tag{13}$$

Equations (12) and (13) show that rotor flux and torque oscillate at the grid frequency, corresponding to the pulsation $\omega_s=2.\pi f_s$. This result is confirmed through the simulation in Figure 2 where $k_1 = 0.1.I_{s1nom}$. Note that from (12) and (13) oscillations amplitude depend on the amplitude of the fault (here k_1). The more the fault is important the more the oscillations are of higher amplitude for the flux as well as for the torque.

3.2. Scaling error

When the current sensors are affected with scaling fault, the error is expressed by equation (14).

$$\Delta I_{si} = k_i.I_{si} \tag{14}$$

With $i \in \{1,2,3\}$

Using (7), (9), (11) and (14), errors on rotor flux and torque are expressed in (15) and (16).

$$\begin{cases} \Delta\Phi_{r\alpha} = \sqrt{\frac{3}{2}}.M_{sr}.K_1.\left|I_s\right|.\cos\theta.\sin\theta_s \\ \Delta\Phi_{r\beta} = -\sqrt{\frac{3}{2}}.M_{sr}.K_1.\left|I_s\right|.\sin\theta.\sin\theta_s \end{cases} \tag{15}$$

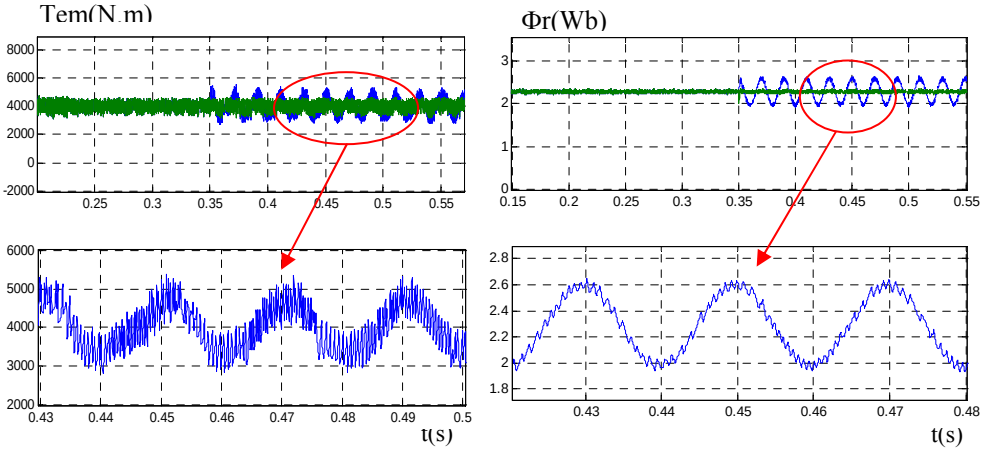

(a) (b)

Figure 2: offset error on *Is1* sensor: effect on (a) Torque and (b) rotor flux

$$\Delta T_{em} = -\frac{3}{4}.p.M_{sr}.K_1.\left|I_s\right|.\left|I_r\right|.\sin 2\theta_s \tag{16}$$

In this case, the expression of the flux modulus error is less evident to calculate. The error obeys to a second order equation given by (17).

$$\Delta\left|\Phi_r\right|^2 + 2.\left|\Phi_r\right|.\Delta\left|\Phi_r\right| - \frac{k^2}{2}.\cos 2\theta_s - k.\left|\Phi_r\right|.\sin 2\theta_s - \frac{k^2}{2} = 0 \quad (17)$$

Where $k = k_1.\left|I_s\right|.M_{sr}.\sqrt{\frac{3}{2}}$.

The solution is oscillatory with a frequency equal to $2.f_s$ which can be verified in Figure 2 where $k_1 = 5\%$. The expression of torque error (Equation (16)) shows oscillations of small amplitude with a frequency of $2.f_s$.This result is also confirmed by the simulation presented in Figure 2. Note that in case of scaling error, currents are obviously deteriorated and equation (11) does not represent correctly the current waveforms which are distorted due to harmonics. This explains the fact that the oscillations of rotor flux are not sinusoidal contrarily to the case of offset error (currents are still sinusoidal thus fairly expressed by (11)). In both fault types, the error affects the estimation. These errors are compensated by the control therefore the effect of the fault is seen on real torque and rotor flux. This is illustrated in figure 2 where blue curves present real variables on the generator and green curves are the estimated ones. These oscillations seen on the electromagnetic torque of the generator are of low harmonics (f_s for offset error and $2.f_s$ for scaling error) are harmful from one hand because they can cause mechanical resonances, from the other hand, they affect the quality of power P_s injected to the grid (P_s is proportional to the torque).

4. DETECTION AND ALGORITHM RECONFIGURATION

4.1. Algorithm reconfiguration

When a sensor fault occurs, a remedial solution is to estimate the quantities initially measured. For the Direct Torque Control, electromagnetic torque and rotor flux are estimated using measured rotor and stator currents. Once the fault is detected, the control algorithm is reconfigured depending on whether the fault is on the rotor or stator side. In the first case, stator currents are estimated whereas in the second case rotor currents are estimated.

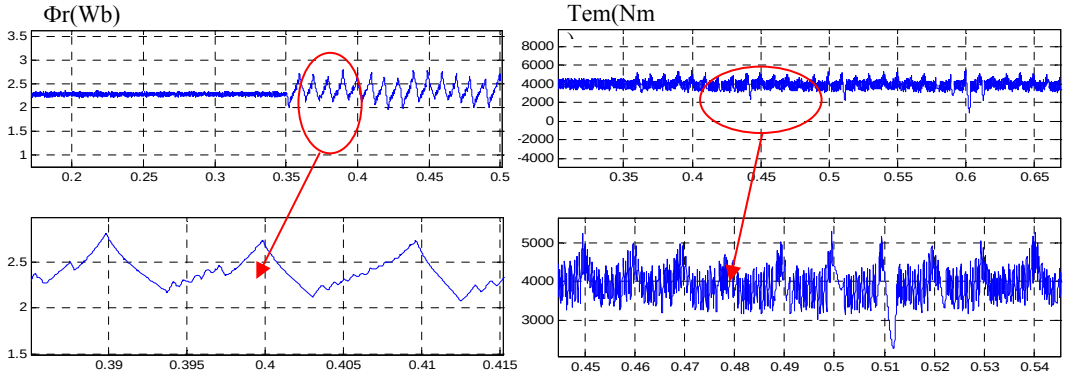

(a) (b)

Figure 3: 5% scaling error on I_{s1} sensor: effect on (a) Torque and (b) rotor flux

The equations used to estimate the rotor flux and the electromagnetic torque are given by (16), (17) where the reference frame is aligned along the stator voltage position which implies that $V_{sq} = 0$ and $V_{sd} = V_s$

Here only stator current sensors failure are treated. The measured stator currents are replaced by estimated currents using equations (18.a), (18.b) and (18.c).

$$\begin{cases} I_{sd\_est} = -\dfrac{M_{sr}}{L_s}.I_{rd\_mes} \\ I_{sq\_est} = -\dfrac{V_{sd\_mes}}{L_s.\omega_s} - \dfrac{M_{sr}}{L_s}.I_{rq\_mes} \end{cases} \quad (18.a)$$

Where

$$\begin{pmatrix} I_{rd\_mes} \\ I_{rq\_mes} \end{pmatrix} = P(-\theta_r).\begin{pmatrix} I_{r\alpha\_mes} \\ I_{r\beta\_mes} \end{pmatrix} \quad (18.b)$$

Then

$$\begin{pmatrix} I_{s\alpha\_est} \\ I_{s\beta\_est} \end{pmatrix} = P(\theta_s).\begin{pmatrix} I_{sd\_est} \\ I_{sq\_est} \end{pmatrix} \quad (18.c)$$

With $P(\phi) = \begin{pmatrix} \cos\phi & -\sin\phi \\ \sin\phi & \cos\phi \end{pmatrix}$, and $\phi = \theta_s$ or $\phi = \theta_r$

The flux components and torque ($\Phi_{r\alpha\_r}, \Phi_{r\beta\_r}, T_{em\_r}$) are estimated using the same equations (2) and (4) replacing measured stator currents by estimated currents.

$$\begin{cases} \Phi_{r\alpha\_r} = L_r.I_{r\alpha\_mes} + M_{sr}.\left(I_{s\alpha\_est}.\cos\theta + I_{s\beta\_est}.\sin\theta\right) \\ \Phi_{r\beta\_r} = L_r.I_{r\beta\_mes} + M_{sr}.\left(I_{s\beta\_est}.\cos\theta - I_{s\alpha\_est}.\sin\theta\right) \end{cases} \quad (19)$$

$$T_{em\_r} = p.\left(\Phi_{r\alpha\_r}.I_{r\beta\_mes} - \Phi_{r\beta\_r}.I_{r\alpha\_mes}\right) \quad (20)$$

Figure 4.a shows the effectiveness of the reconfiguration. Here, the fault occurs at t=0.3s and the control is reconfigured at t=0.4s in order to point out the change in torque and flux waveforms but in practice the system needs only one sampling period to detect and reconfigure the control.

4.2. FAULT DETECTION AND ISOLATION

The idea of the detection method is to compare the difference between measured and estimated currents [7]. Three current sensors are used, instead of two as commonly done. Indeed, for high power system like wind systems, reliability considerations are more important than cost considerations. The method is applied here in the case of faulty stator sensors and it can be extended in the same way to rotor sensors. The $\alpha\beta$ current components

are used to isolate the three cases where only one sensor is faulty. The estimated $\alpha\beta$ currents

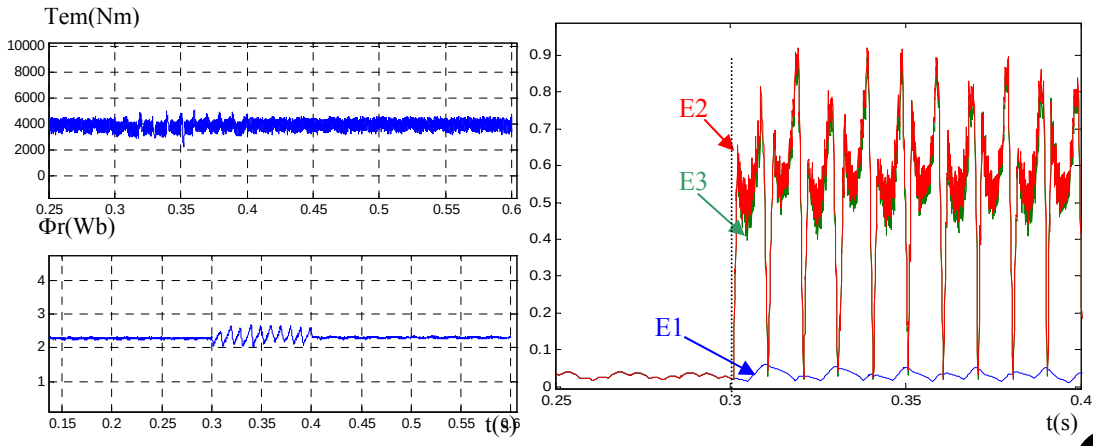

(a) (b)

Figure 4: Scaling error on Is1 sensor: (a) torque and rotor flux before and after reconfiguration (b) calculated errors

are calculated using equations (18.a), (18.b) and (18.c) when one of stator sensors is faulty (respectively analog equations when rotor sensors are faulty).The measured $\alpha\beta$ currents are calculated replacing the faulty sensor using the relation

$$i_{s1} + i_{s2} + i_{s3} = 0 \tag{21.a}$$

If sensor of phase 1 is faulty then:

$$i_{s1\_f} = -i_{s2\_mes} - i_{s3\_mes} \tag{21.b}$$

$$\begin{bmatrix} i_{s\alpha\_f} \\ i_{s\beta\_f} \end{bmatrix} = \begin{pmatrix} \sqrt{\frac{3}{2}} & 0 & 0 \\ \frac{1}{\sqrt{2}} & \sqrt{2} & 0 \end{pmatrix} \cdot \begin{bmatrix} i_{s1\_f} \\ i_{s2\_mes} \\ i_{s3\_mes} \end{bmatrix} \tag{21.c}$$

The error is calculated as follows:

$$E_1 = \left| i_{s\alpha\_f} - i_{s\alpha\_est} \right| + \left| i_{s\beta f} - i_{s\beta\_est} \right| \tag{22}$$

If sensor 1 is faulty then E_1 is small. In the same way E_2 and E_3 are calculated. The isolation of the faulty sensor is made through the calculation of the minimum of E_1, E_2 and E_3. Effectively, Figure 4.b presents E_1, E_2 and E_3 when the sensor of stator phase 1 is faulty. The detection can be done since the first sampling period after the occurrence of the fault when the three errors are no more equals but the detection can take more time due to measure and modulation noise. The main idea is to reconfigure the algorithm as soon as the fault is detected to ensure the continuity of working. The faulty sensor can be isolated few sampling periods after the fault detection. Once the isolation is done, the algorithm can

move to a two sensors system using equation (21.a) without any other modification of the control algorithm. This last point underlines the importance of fault isolation in control reconfiguration since only one simple equation needs to be programmed in order to ensure the same performances for the system as before the occurrence of the fault.

5. CONCLUSION

Current sensor failures have been studied in this work. Two faults were treated namely offset and scaling error. A sensibility analysis has been presented to underline the effect of these faults on the Direct Torque Control of a DFIG based VSWS. Sensors redundancies of this system have been exploited to reconfigure system control after the fault detection. Low harmonics torque oscillations are the major problem because they may cause mechanical resonances but also ripples in the power injected to the grid. The simulation results show the effectiveness of the detection and isolation method and of control reconfiguration as a remedy for this type of faults.

References

[1] Saccomando G., Svensson J., Sannino A.,'Improving Voltage Disturbance Rejection for Variable-Speed Wind Turbines'. IEEE Transactions On Energy Conversion, Vol.17, No.3, pp.422-428, September 2002.

[2]] Niiranen J. 'Voltage dip ride through of a doubly-fed generator equipped with an active Crowbar'. Nordic wind power conference, 1-2 March 2004, Chalmers university of technology.

[3] Rogério G. de Almeida, J. A. Peças Lopes J. A. L. Barreiros, 'Improving Power System Dynamic Behavior Through Doubly Fed Induction Machines Controlled by Static Converter Using Fuzzy Control', IEEE TRANSACTIONS ON POWER SYSTEMS, VOL. 19, NO. 4, NOVEMBER 2004, pp1942-1950.

[4] Akhmatov V., 'Variable-Speed Wind Turbines with Doubly-Fed Induction Generators'. Wind Engineering Vol.26 ,No.2, pp.85-108, 2002.

[5] L.Laurila, P.Kurronen, M.Niemela, J.Pyrhonen,'Effect of unideal current sensors in direct torque controlled PMSM drives', NORpi2002, Nordic Workshop on Power and Industrial Electronics, Stockholm, Sweden, August 2002.

[6] Jihen, A., Slama-Belkhodja, I., 'Investigation of fault tolerant of direct torque control in induction motor drive' IEEE Conference on Power Electronics and Machine Drives, PEMD'04, Volume 1 pp. 67 – 72, Mars 2004, Edingburg,UK.

[7] L.Baghli, P.Poure, A.Rezzoug, 'Sensor fault detection for fault tolerant vector controlled induction machine', EPE2005, 11th European Conference on Power Electronics and Applications, September, 11-14, 2005, Dresden, Germany.

[8] H.S.Jung, J.M.Kim, C.U. Kim, 'Diminution of current measurement error for vector controlled AC motor drives', IEMDC2005, IEEE-International Electric Machines and Drives Conference, May ,2005, San Antonia, Texas, USA.

[9] Arnaltes S.,Burgos J.C, Rodriguez-Amenedo J.L, 'Direct Torque Control of a Doubly-Fed Induction Generator for Variable Speed WindTurbines', Electric Power Components andSystems,Vol.30, No.2, pp.199-216, February 2002.

[10] E.Favre, W.Teppan, 'State-of-Art in current sensing technologies', PCIM'03, May 20-22**,** Nuremberg, Germany

[11] Dongyuan Qiu, S.Y. R. Hui, H. S. H. Chung, **'**Some Practical Issues Related to Inductor Model in Single-Sensor Measurement Technique', 35th Annual IEEE Power Electronics Specialists Conference Aachen, Germany, 2004.

[12] Pena R., Clare J.C, Asher G.M, 'Doubly fed induction generator using back-to-back PWM converters and its application to variable-speed wind-energy generation'. IEE Proc-Electr. Power Appl. Vol.143, No. 3, pp.231-241, May 1996.